

# Resonant x-ray scattering from chiral materials: $\alpha$ -quartz, $\alpha$ -berlinite, and tellurium

Manabu Takahashi<sup>1</sup>, Jun-ichi Igarashi<sup>2</sup>

<sup>1</sup> Faculty of Science and Technology, Gunma University, Kiryu, Gunma 376-8515, Japan

<sup>2</sup> Faculty of Science, Ibaraki University, Mito, Ibaraki 310-8512, Japan

E-mail: mtakahas@gunma-u.ac.jp

**Abstract.** We study the resonant x-ray scattering (RXS) at Si K, Al K and Te L1-edges from chiral materials,  $\alpha$ -quartz,  $\alpha$ -berlinite, and tellurium. For the forbidden reflections (001) and (00 $\bar{1}$ ), we deduce the scattering matrix for the E1E1 event by summing up the local scattering matrices. The oscillation terms proportional to  $\cos(3\Psi \mp \delta)$  and  $\sin(3\Psi \mp \delta)$  are obtained in the spectral intensity as a function of azimuthal angle  $\Psi$  with an expression of possible phase shift  $\delta$ . We evaluate the parameters which cannot be determined in the symmetry argument on the basis of underlying electronic structures given by the bond-orbital model calculation for  $\alpha$ -quartz and  $\alpha$ -berlinite, and by using the FLAPW band structure calculation based on the local density approximation for tellurium. The calculated spectra reproduce well the experimental results which depend on photon polarization and crystal chirality. We point out that the finite core-hole life-time and the band effect in the intermediate states may cause together the phase shift  $\delta$ .

## 1. Introduction

Alpha-quartz (SiO<sub>2</sub>), alpha-berlinite (AlPO<sub>4</sub>), and tellurium (Te) are chiral materials, having two stereoisomeric crystal forms, the right-handed screw (space group No.152,  $P3_121$ ) and the left-handed screw (No.154,  $P3_221$ ). The two forms have been distinguished by using the optical activity since the discovery of Arago and Biot [1]. In order to determine the atomic positions for systems with different chirality, the anomalous x-ray scattering has been utilized [2, 3].

Recently, another method has been attempted to distinguish chirality: the resonant x-ray scattering (RXS) with circularly polarized beam [4, 5, 6], using the Si K, Al K, and Te L1-edge resonances in  $\alpha$ -quartz,  $\alpha$ -berlinite, and tellurium, respectively. The tensor character of scattering matrix of RXS could give rise to the intensity on the reflections forbidden in Thomson scattering [7, 8, 9]. Measuring the spectra on the forbidden reflections (001) and (00 $\bar{1}$ ), Tanaka et al. [4, 5, 6] have found characteristic patterns depending on chirality in the spectral intensity by means of switching polarizations from the right-handed one (RCP) to the left-handed one (LCP). Regarding the oscillation of the intensity as a function of azimuthal angle, interesting phase shift has been also observed. The amount of the phase shift strongly depends on the excitation energy. It has been suggested that the phase shift might be due to the interference between the parity even E1E1 and the parity-odd E1E2 or E1M1 events [4, 5, 6]. As a possible mechanism for the phase shift, the birefringence might not be ignored. Joly et al pointed out the importance of the birefringence effect on the analysis of the Cu  $L$  edge RXS spectra from cupric oxide [10].



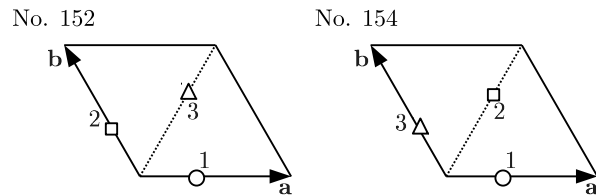


**Figure 1.** Si, Al, or Te atoms projected onto the  $a$ - $b$  plane in the unit cell. Atoms labeled by 1, 2, 3 are located at  $(u, 0, 0)$ ,  $(0, u, \frac{1}{3})$ ,  $(1-u, 1-u, \frac{2}{3})$  for No. 152, and at  $(u, 0, 0)$ ,  $(1-u, 1-u, \frac{1}{3})$ ,  $(0, u, \frac{2}{3})$  for No. 154, respectively.

In this paper we discuss the dependence of the RXS intensity from chiral materials on the crystal chirality, Bragg reflection, and incident photon polarization. For the forbidden reflections  $(001)$  and  $(00\bar{1})$ , we deduce the general form of the scattering matrix for the E1E1 event obtained by summing up the local scattering matrices. The oscillation term proportional to  $\cos(3\Psi \mp \delta)$  and  $\sin(3\Psi \mp \delta)$  is obtained in the spectral intensity as a function of azimuthal angle  $\Psi$  with an expression of possible phase shift  $\delta$ . We demonstrate for tellurium that the phase shift could be related to the core-hole life-time and the band effect in the intermediate states as well as the effects of the parity-odd events and the birefringence. The present paper is organized as follows. In Sec. 2, the crystal symmetry and the formula of the RXS intensity are briefly described. In Sec. 3, the calculated results are discussed. Sec. 4 is devoted to the concluding remarks.

## 2. Crystal Symmetry and Formula of the RXS

Bravais lattice of  $\alpha$ -quartz,  $\alpha$ -berlinite, and tellurium is hexagonal. As shown in Fig. 1, Si, Al, or Te atom sits at the positions  $(u, 0, 0)$ ,  $(0, u, \frac{1}{3})$ ,  $(1-u, 1-u, \frac{2}{3})$  for No.152, while at the positions  $(u, 0, 0)$ ,  $(1-u, 1-u, \frac{1}{3})$ ,  $(0, u, \frac{2}{3})$  for No.154, where  $u = 0.47, 0.47, \text{ and } 0.26$ , for Si, Al, and Te, respectively. The  $a$ -axis is a two-fold rotation axis for both No.152 and No.154, and that the crystal of No.154 is the mirror image of No.152 with respect to the  $a$ - $b$  plane.

We construct the resonant scattering matrix based on the symmetry. We briefly summarize the derivation of formula for the RXS intensity. For the detailed derivation we refer the readers to ref. [11]. Let the incident and scattered photon polarizations be specified as  $x_\beta$  and  $x_\alpha$  in Cartesian frame that the  $x_1(\equiv x)$  and  $x_3(\equiv z)$  axes are along the  $a$  and  $c$  axes of the hexagonal lattice. We introduce the local dipole-dipole correlation function at the core-hole site  $j$  excited by absorbing an incident photon, which is defined by

$$[\hat{\rho}_j(\epsilon)]_{\alpha,\beta} = \sum_n \langle g | \hat{x}_\alpha | n \rangle \langle n | \hat{x}_\beta | g \rangle \delta(\epsilon + \epsilon_g - \epsilon_n), \quad (1)$$

where the dipole operator  $\hat{x}_\alpha$  is measured from the nuclear position of site  $j$ . Ket  $|g\rangle$  represents the ground state with energy  $\epsilon_g$ , and  $|n\rangle$  represents the intermediate state with energy  $\epsilon_n$ . Let the local dipole-dipole correlation function at site  $(u, 0, 0)$  be  $\hat{\rho}_1^{(\pm)}$  with  $+$  and  $-$  signs corresponding to No.152 and No.154. It takes the following matrix form according to the local symmetry:

$$\hat{\rho}_1^{(\pm)}(\epsilon) = \begin{pmatrix} a(\epsilon) & 0 & 0 \\ 0 & b(\epsilon) & \pm d(\epsilon) \\ 0 & \pm d(\epsilon) & c(\epsilon) \end{pmatrix}, \quad (2)$$

where  $a(\epsilon)$ ,  $b(\epsilon)$ ,  $c(\epsilon)$ , and  $d(\epsilon)$  are real functions of energy  $\epsilon$ . The presence of the off-diagonal elements is due to the lack of inversion symmetry around the Si, Al, and Te atoms. The zero

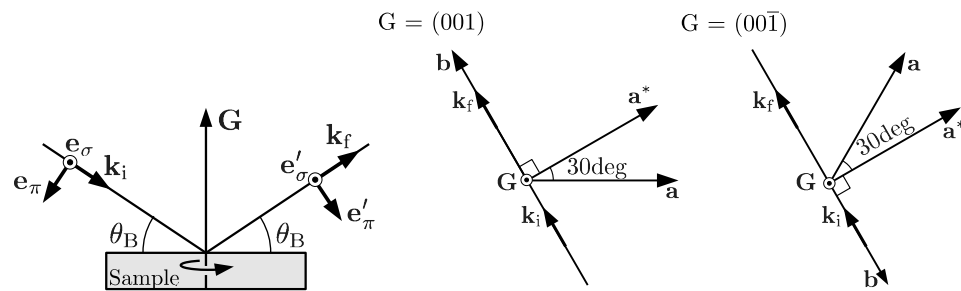


**Figure 2.** Scattering geometry. Left : Side view of the scattering geometry. The unit vector for the  $\sigma$  and  $\pi$  polarizations are defined as shown. Center : Top view of the scattering geometry at the azimuthal angle  $\Psi = 0$  for  $\mathbf{G} = (001)$ , looking *down* along the  $c$  axis from the top of the axis. Right : Top view for  $\mathbf{G} = (00\bar{1})$ , looking *up* along the  $c$  axis from the bottom of the axis. Vectors  $\mathbf{a}$  and  $\mathbf{b}$  are translational vectors along the  $a$  and  $b$  axes, respectively. Vector  $\mathbf{a}^*$  is the reciprocal lattice vector conjugate to  $\mathbf{a}$ .

components are originated from the two-fold rotation symmetry around the  $a$ -axis. The  $\pm$  signs are originated from the mirror-image relation with respect to the  $a$ - $b$  plane between No.152 and No.154. The elements  $a(\epsilon)$ ,  $b(\epsilon)$ ,  $c(\epsilon)$ , and  $d(\epsilon)$  are determined on the basis of underlying electronic structure. The local correlation function  $\hat{\rho}_{2(3)}^{(\pm)}(\epsilon)$  on the atomic site 2(3), are obtained by rotating  $\hat{\rho}_{1}^{(\pm)}(\epsilon)$  by  $\pm 2\pi/3$  ( $\mp 2\pi/3$ ) around the  $c$ -axis. We may express the total resonant scattering matrix for scattering vector  $\mathbf{G} = \mathbf{k}_f - \mathbf{k}_i$  as

$$\hat{M}(\mathbf{G}; \omega) = \sum_j \int \frac{\hat{\rho}_j(\epsilon) \exp(-i\mathbf{G} \cdot \mathbf{r}_j)}{\omega - \epsilon + i\Gamma} d\epsilon, \quad (3)$$

where  $\mathbf{k}_i$  and  $\mathbf{k}_f$  are the wave vectors for the incident and scattered x-rays, respectively. The scattering geometry is shown in fig. 2. For  $\mathbf{G} = (00\bar{1})$ , the total resonant scattering matrix is written as

$$\hat{M}((00\bar{1}); \omega) \begin{pmatrix} A(\omega) & \mp iA(\omega) & -iB(\omega) \\ \mp iA(\omega) & -A(\omega) & \pm B(\omega) \\ -iB(\omega) & \pm B(\omega) & 0 \end{pmatrix}, \quad (4)$$

with

$$A(\omega) = \frac{3}{4} \int \frac{a(\epsilon) - b(\epsilon)}{\omega - \epsilon + i\Gamma} d\epsilon, \quad (5)$$

$$B(\omega) = \frac{3}{2} \int \frac{d(\epsilon)}{\omega - \epsilon + i\Gamma} d\epsilon, \quad (6)$$

where  $\omega$  and  $\Gamma$  represent the photon energy and the life-time broadening width of the core hole state, respectively. We note that  $A(\omega)$  and  $B(\omega)$  are complex functions, and generally linear independent of each other. The matrix for  $\mathbf{G} = (001)$  is obtained by changing the sign before the pure imaginary constant  $i$  in eq. (4).

We rotate the crystal right-handedly around  $\mathbf{G}$  with azimuthal angle  $\Psi$ . Following the experimental setup by Tanaka et al., [4, 6] we define the origin of  $\Psi$  such that the scattering plane contains the  $b$  axis, as shown in Fig. 2.

In the case that the incident beam is circularly polarized and the polarization of scattered x-ray is not detected, the scattering intensity may be expressed in the following form using Stokes

parameters  $P_1$ ,  $P_2$ , and  $P_3$  [12]:

$$I((00\bar{1});\omega) = I_0 - I_1 \sin(3\Psi \mp \delta) - I_2 \cos(3\Psi \mp \delta), \quad (7)$$

with

$$I_0 = |B|^2 \cos^2 \theta_B + |A|^2 \frac{1 + \sin^2 \theta_B}{2} \times (1 + \sin^2 \theta_B \pm 2P_2 \sin \theta_B + P_3 \cos^2 \theta_B), \quad (8)$$

$$I_1 = |AB| \cos \theta_B (P_2 \cos^2 \theta_B \mp 2P_3 \sin \theta_B), \quad (9)$$

$$I_2 = \mp |AB| \cos \theta_B (1 + \sin^2 \theta_B) P_1. \quad (10)$$

where the upper (lower) sign corresponds to the crystal of No.152 (No.154), and  $B^*A$  is replaced by  $|AB|e^{i\delta}$ .  $I((001);\omega)$  is obtained by changing the sign before  $I_1$  and  $I_2$  in eq. (7). Right(Left) circularly polarization correspond to  $P_2 = +1(-1)$ . We note that the phase  $\delta$  could take any value in principle. If  $A(\omega)$  and  $B(\omega)$  are linearly dependent on each other,  $\delta$  can only take 0 or 180 deg because  $B^*A$  takes positive or negative real value. In case of  $P_1 = 0$ , the oscillating term as a function of azimuthal angle  $\Psi$  consist only of the term proportional to  $\sin(3\Psi \mp \delta)$ .

### 3. Calculated Results and Discussions

In order to determine the parameters  $a(\epsilon)$ ,  $b(\epsilon)$ ,  $c(\epsilon)$ , and  $d(\epsilon)$ , we exploit the bond-orbital model for  $\alpha$ -quartz and  $\alpha$ -berlinite [11], which are insulators with a wide energy gap. We make use of the FLAPW band structure calculation based on the local density approximation (LDA) for tellurium, which is a semiconductor with a tiny band gap  $\sim 0.3\text{eV}$ . For  $\alpha$ -quartz and  $\alpha$ -berlinite, the FLAPW calculation ignoring the core-hole potential fails to reproduce the observed absorption spectral curves. On the other hand, for tellurium, the FLAPW calculation rather well reproduce the observed absorption spectral curve. Therefore, one particle approximation based on the LDA calculation ignoring the core-hole potential is expected to work safely for discussing the nature of the RXS spectra in tellurium. In the one particle approximation, the local dipole-dipole correlation function  $\hat{\rho}_j(\epsilon)$  may be calculated from the single particle density matrix projected on the  $p$ -symmetric states at the scattering site. Each element in the density matrix can be explicitly expressed in terms of the FLAPW basis.

We concentrate our attention on the azimuthal angle dependence of the spectral intensity at the  $\omega$  giving the main absorption peak for  $\mathbf{G} = (00\bar{1})$  for  $\alpha$ -quartz and  $\alpha$ -berlinite belonging to No. 154. Figure 3 shows the RXS intensity as a function of azimuthal angle  $\Psi$  comparing with the observed ones in  $\alpha$ -quartz and  $\alpha$ -berlinite [4, 5]. Although  $\mathbf{G}$  is defined by  $\mathbf{k}_i - \mathbf{k}_f$  in the experiment, which is opposite to ours (see the errata in Ref. [4]), we present  $\mathbf{G}$ 's in our definition. The calculated intensities are smaller for RCP than those for LCP in No.154, being consistent with the experimental curves shown in panels (b) and (d), while the former is larger than the latter in No.152 (not shown). As regards the oscillation terms, we notice from the eqs. (7) and (9) that they take the form of  $-a_1 \sin(3\Psi - \delta)$  for RCP in No.152, and  $a_1 \sin(3\Psi + \delta)$  for LCP in No.154 with  $a_1$  a positive number, and that they take the form of  $b_1 \sin(3\Psi - \delta)$  for LCP in No.152, and  $-b_1 \sin(3\Psi + \delta)$  for RCP in No.154 with  $b_1$  a positive number. Their ratio is given by  $b_1/a_1 = (|P_2| \cos^2 \theta_B + 2P_3 \sin \theta_B) / (|P_2| \cos^2 \theta_B - 2P_3 \sin \theta_B) \sim 0.2$  for  $\alpha$ -quartz and  $\sim 1.71$  for  $\alpha$ -berlinite, which is independent of the model. These values are quite well consistent with the observed ones. However, there are noticeable discrepancies between the calculation and the experiments. In  $\alpha$ -quartz, the intensities for RCP in No.154 are too small in comparison with the experiment. Concerning the phase shift, the experimental curves in  $\alpha$ -quartz seems to have the phase shift  $\delta = 120 \sim 180$  deg. It is also reported that the phase shift depends on the photon energy  $\omega$  in  $\alpha$ -quartz and  $\alpha$ -berlinite. Although the phase  $\delta$  in eq. (7) could take any value in

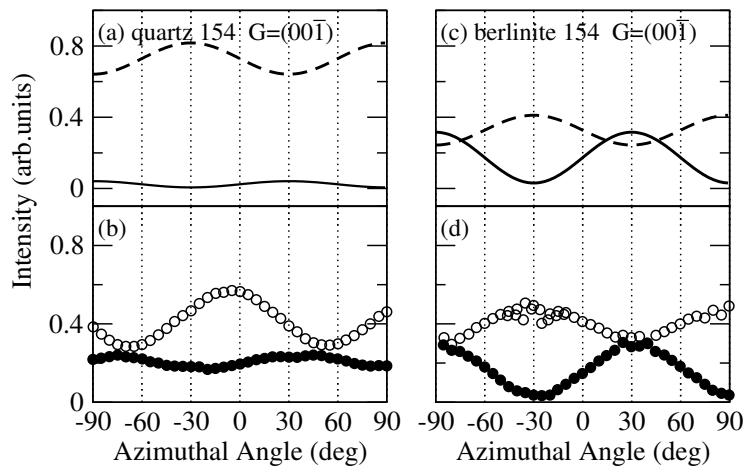


**Figure 3.** RXS intensity from  $\alpha$ -quartz and  $\alpha$ -berlinite of No.154, for  $\mathbf{G} = (00\bar{1})$ . The  $\omega$  is fixed at the value giving the absorption peak (not shown).  $P_1 = 0$ ,  $P_3 = -0.31$ ,  $P_2 = 0.95$  (RCP), and  $P_2 = -0.95$  (LCP) and  $\sin \theta_B = 0.625$  for quartz, and  $P_1 = 0$ ,  $P_3 = +0.30$ ,  $P_2 = 0.95$  (RCP), and  $P_2 = -0.95$  (LCP), and  $\sin \theta_B = 0.361$  for berlinite. Lower panel shows the experimental curves reproduced from Refs. [4] and [5]. Solid curves and solid circles are for RCP, and dashed curves and open circles are for LCP.

principle, the bond-orbital model gives the phase shift  $\delta = 180$  deg. independent of the photon energy. This is may caused by the fact that the four  $sp^3$  hybrid orbitals on the scattering site are assumed not to interact with each other in our bond-orbital model, which leads to the result that  $A(\omega)$  and  $B(\omega)$  are linearly dependent on each other. The most serious discrepancy is that the phase shift in  $\alpha$ -quartz looks to depend on the photon polarization and the Bragg reflection  $\mathbf{G}$  [4], although the phase shift  $\delta$  should be independent of them in accordance with the symmetry argument within the E1E1 approximation.

In accordance with eqs. (5) and (6), the energy dependent phase shift  $\delta$  is expected to be caused by the life-time broadening  $\Gamma$  of the core hole and the band effect on the intermediate states. In order to elucidate these effects, we adopt the FLAPW band structure calculation for tellurium to evaluate the parameters  $a(\epsilon)$ ,  $b(\epsilon)$ ,  $c(\epsilon)$ , and  $d(\epsilon)$ . We assume the life-time broadening for Te 2s core hole state  $\Gamma = 1.5$  eV [13]. Figure 4 shows the calculated absorption and RXS intensities as a function of photon energy  $\omega$  at  $\Psi = 0$ , reproducing well the observed spectral shape [6]. The absorption spectra show a peak structure near the edge and broad structures in higher energy region. On the other hand, RXS spectra show almost single peak structure with small shoulder structures in higher energy region. The calculated phase shift  $\delta$  is found to strongly depend on the photon energy as shown in the figure 4(center). The phase shift at the photon energy giving the RXS peak intensity is  $\delta \sim 196$  deg, which is nearly equal to the observed value  $\delta_{\text{exp}} \sim 194$  deg. The calculated intensities are slightly smaller for RCP than for LCP in No.154 and the ratio  $b_1/a_1$  equals to 1. These are well consistent with the observations.

#### 4. Concluding Remarks

We have analyzed the RXS spectra at Si and Al K-edges and Te L1-edge on forbidden reflections in chiral materials,  $\alpha$ -quartz,  $\alpha$ -berlinite, and tellurium, using the expressions of scattering matrix for the E1E1 event. The expressions include the oscillation term as a function of azimuthal angle, which has the phase shift and the amplitude with chirality dependence.

The calculated spectra based on the bond orbital model have reproduced well main aspect of the experimental observations  $\alpha$ -quartz and  $\alpha$ -berlinite. However, some discrepancies remain in

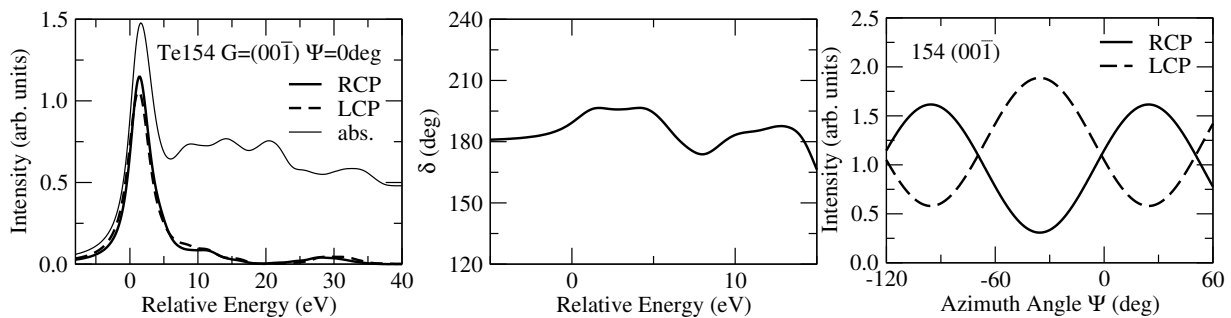


**Figure 4.** Calculated absorption and RXS intensities as a function of photon energy (left), phase shift  $\delta$  as a function of photon energy (center), and RXS peak intensity as a function of azimuthal angle (right) in tellurium of No.154 for  $\mathbf{G} = (00\bar{1})$ . The energy zero corresponds to the energy difference between Te 2s level and the conduction band bottom. The life-time broadening is chosen as  $\Gamma = 1.5$  eV.  $P_1 = 0$ ,  $P_3 = 0$ ,  $P_2 = 1$  (RCP), and  $P_2 = -1$  (LCP) and  $\sin\theta_B = 0.212$ . Solid and dashed curves are for RCP, and LCP, respectively. The azimuthal angle zero in the experiment corresponds to  $\Psi = -90$  deg.

the average intensities and the phase shift of azimuthal angle oscillation in  $\alpha$ -quartz. The phase shift depending on the photon energy has not been explained within the bond orbital model calculation. On the other hand, for tellurium the calculated spectra based on the band structure calculation have well reproduced the observations. We have demonstrated that the finite core-hole life-time and the band effect in the intermediate states can cause together the energy dependent phase shift  $\delta$  in the azimuthal dependence of the scattering intensity even for the E1E1 event as well as the effects of the parity-odd events and the birefringence. It is interesting that the finite core-hole life-time causes not only the broadening of the spectra but also the phase shift. Using FLAPW band structure calculation to evaluate the dipole-dipole correlation function, and assuming the core-hole life-time broadening  $\Gamma = 1.5$ eV, we have successfully reproduced the absorption and RXS spectra at the Te L1 edge as functions of photon energy, and the azimuthal angle dependence of RXS intensity, including the amount of the phase shift for tellurium. For better understanding the phase shift behavior for  $\alpha$ -quartz and  $\alpha$ -berlinite, further studies taking account of the core hole potential and band effect are required.

## Acknowledgments

This work was partially supported by a Grant-in-Aid for Scientific Research from the Ministry of Education, Culture, Sports, Science and Technology of the Japanese Government.

## 5. References

- [1] For a historical account, see for example, S. F. Mason, *Molecular Optical Activity and the Chiral Discriminations* (Cambridge University Press, 1982).
- [2] Bijvoet J M, Peerdeman A F and van Bommel J A 1951 *Nature* **168** 271
- [3] de Vries A 1958 *Nature* **181** 1193
- [4] Tanaka Y, Takeuchi T, Lovesey S W, Knight K S, Chainani A, Tanaka Y, Oura M, Senba Y, Ohashi H and Shin S 2012 *Phys. Rev. Lett.* **100** 145502(2008); *ibid.* **108**, 019901(E)
- [5] Tanaka Y, Kojima T, Takata Y, Chainami A, Lovesey S W, Knight K S, Takeuchi T, Oura M, Senba Y, Ohashi H and Shin S 2011 *Phys. Rev. B* **81** 144104(2010); *ibid.* **84**, 219905(E)
- [6] Tanaka Y, Collins S P, Lovesey S W, Matsumami M, Moriwaki M and Shin S 2012 *J. Phys.: Condens. Matter* **22** 1220(2010); *ibid.* **24**, 159905(E)
- [7] Templeton D H and Templeton L K 1982 *Acta Crystallogr. A* **38** 62
- [8] Dmitrienko V E 1983 *Acta Crystallogr. A* **39** 29
- [9] Dmitrienko V E, Ishida K, Kirfel A and Ovchinnikova E N 2005 *Acta Crystallogr. A* **61** 481

- [10] Joly Y, Collins S P, Grenier S, Tolentino H C N and Dantis M D 2012 *Phys. Rev. B* **86** 220101
- [11] Igarashi J and Takahashi M 2012 *Phys. Rev. B* **86** 104116
- [12] V. B. Berestetskii, E. M. Lifshitz, and L. P. Pitaevskii, *Quantum Electrodynamics* (Butterworth-Heinemann, 1982), Sec. 8.
- [13] Krause M O and Oliver J H 1979 *J. Phys. Chem. Ref. Data* **8** 329